Multi-messenger astronomy and the extreme Universe

Andrii Neronov

APC Paris & EPFL Lausanne

!!! IMPORTANT information for all participants. Check this link for the latest COVID-19 regulations in Vienna and Austria!!!

There are several open questions in Physics today, each of which touches the fields of both Particle Physics and Astroparticle/Cosmology. For example, only 5% of the Universe is described by the Standard Model of particle physics. A far larger contribution comes from the elusive Dark Matter, whic has been inferred from gravitational and astroparticle measurements. A large variety of models have

– Dark matter
– Baryogenesis and Leptogenesis
– Matter at nuclear densities
– Relativistic gravity theory
– Lorentz invariance, weak equivalence principle
– ....

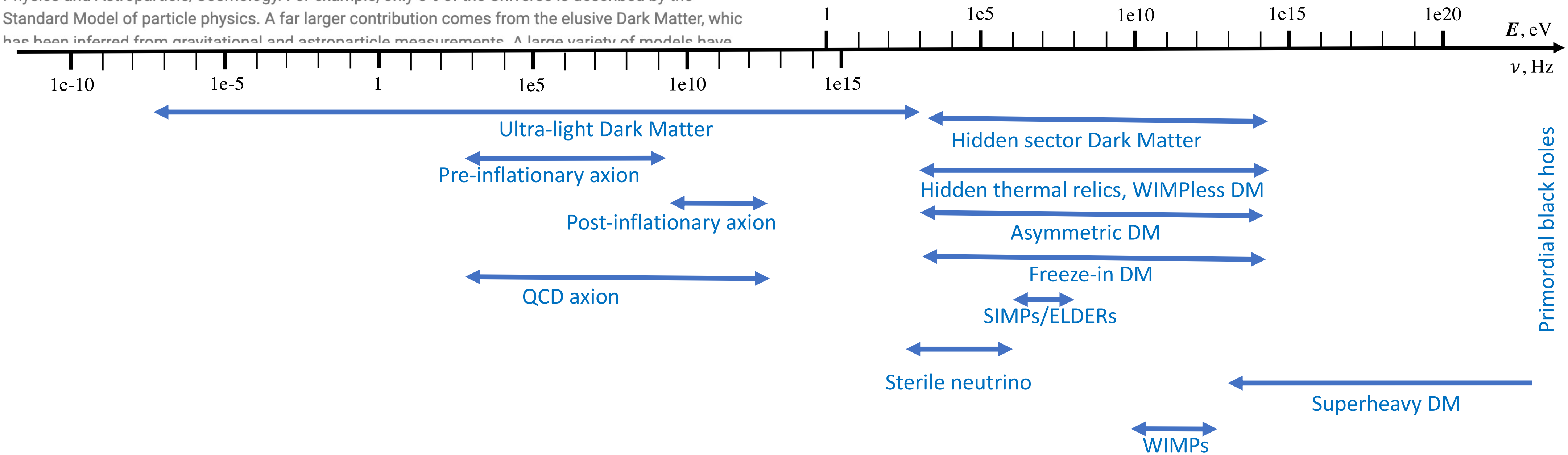

US Cosmic Visions 2017 report: arXiv:1707.04591

Multi-messenger astronomy and the extreme Universe

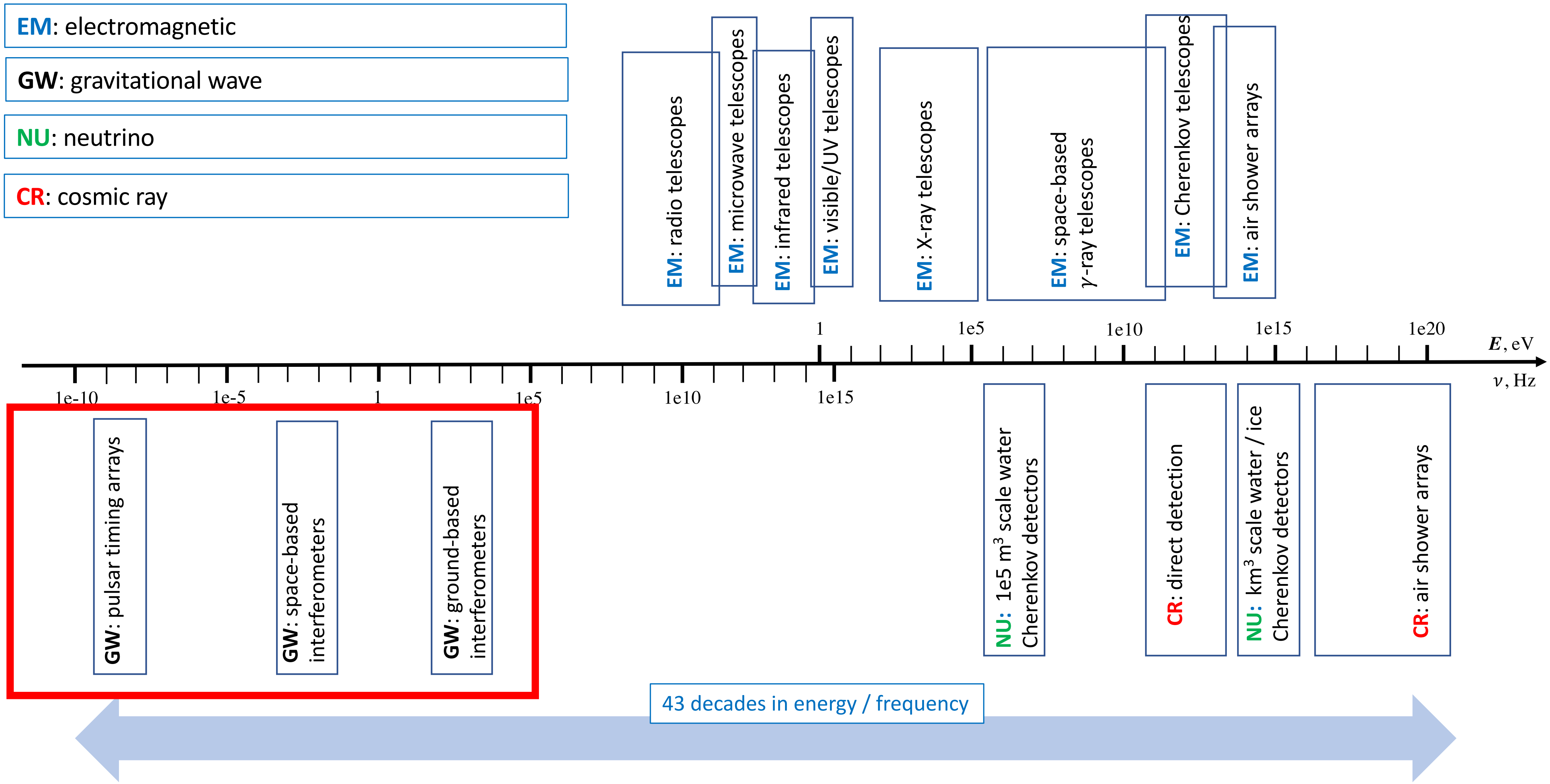

Nano-Hz gravitational waves with Pular Timing Arrays (PTA)

Passage of gravitational waves distorts the pattern of arrival time of pulsars by changing the distance to the sources. Measurement of timing residuals allows to detect gravitational waves with extremely low frequency, down to nHz (low frequency end is determined by the duration of timing monitoring, currently ~ 10 yr scale).

Pulsar timing arrays can detect gravitational waves from binary supermassive black holes forming at galaxy mergers:

$$P = \sqrt{\frac{2\pi R^3}{G_N M}} \simeq 5 \left[\frac{M}{10^7 M_\odot}\right]^{-\frac{1}{2}} \left[\frac{R}{10^{16}\ \mathrm{cm}}\right]^{\frac{3}{2}} \mathrm{yr}; \quad \nu = P^{-1}$$

All PTA collaborations (NANOGrav, EPTA, PPTA, collaborating within "International" PTA, IPTA) have reported evidence for "common stochastic process" detectable in timing residuals of many pulsars. This is consistent with existence of stochastic gravitational wave background, but the definitive test, measurement of the angular dependence of cross-correlation power (Hellings-Downs) is not precise enough.

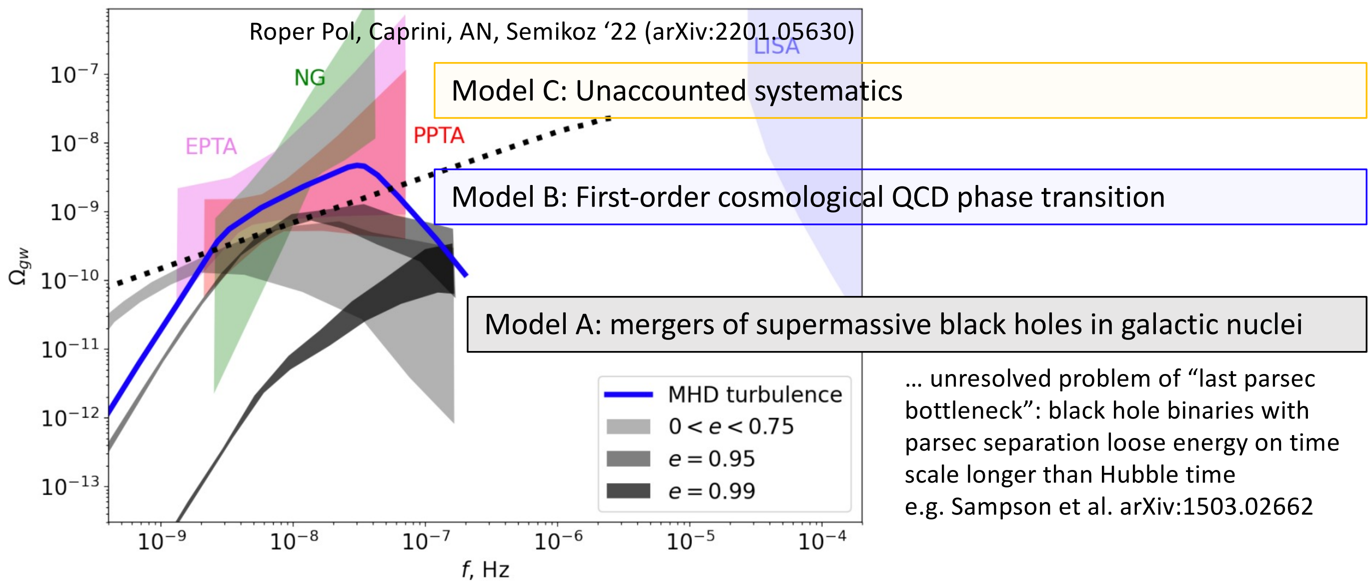

... unresolved problem of "last parsec bottleneck": black hole binaries with parsec separation loose energy on time scale longer than Hubble time e.g. Sampson et al. arXiv:1503.02662

NANOGrav Collab. '20 (arXiv:2009.04496)
PPTA Collab. '21 (arXiv:2107.12112)
EPTA Collab. '21 (arXiv:2110.13184)
IPTA Collab. '22 (arXiv:2201.03980

Fundamental physics with stochastic gravitational wave background(s)

… and cosmological magnetic fields

Within the Standard Model the Electroweak and QCD transitions are expected to cross-overs Detection of relic SGWB in nHz-mHz range would constitute an evidence for beyond-Standard-Model process(?).

1st-order phase transition also generates magnetic field that survives till present epoch as Intergalactic Magnetic Field (IGMF). This field can be measured in the near future via its effect on propagation of gamma-rays, and/or its effect on polarized radio signals and ultra-high-energy cosmic rays and/or its effect on Cosmic Microwave Background.

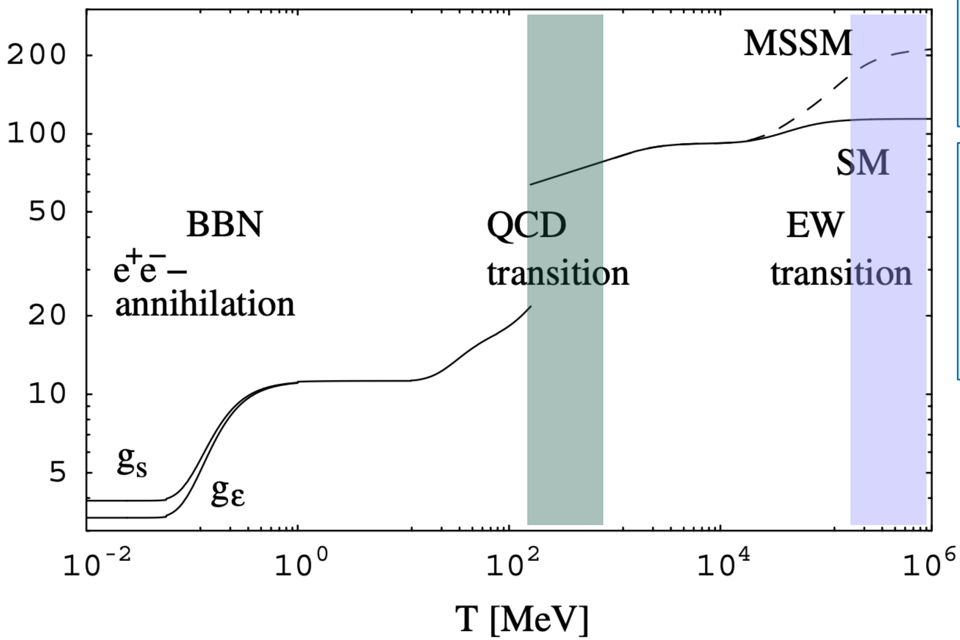

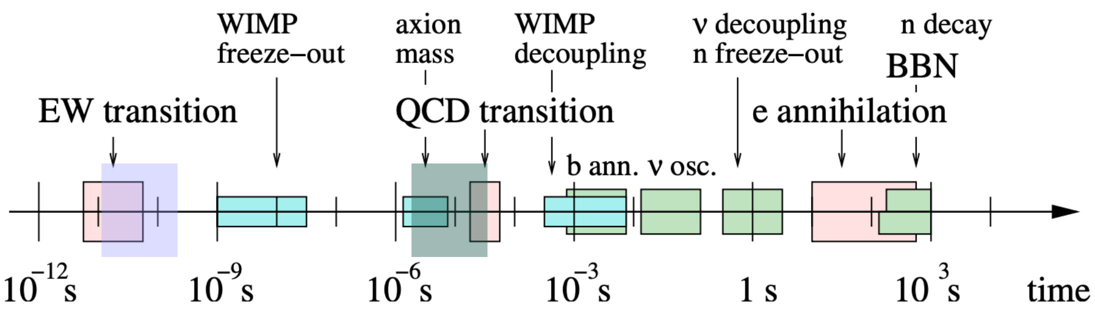

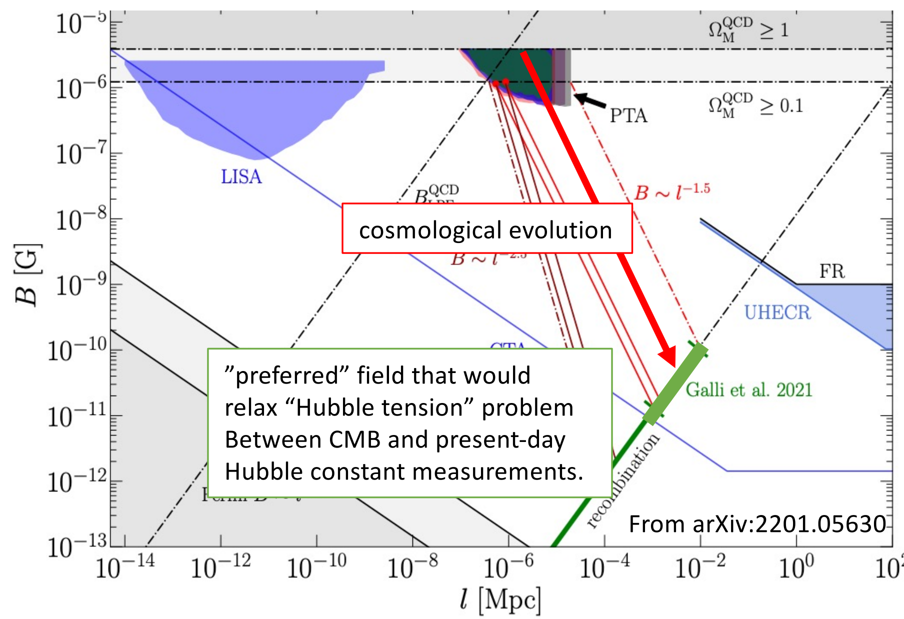

CMS Physics TDR, (DOI: 10.1088/0954-3899/34/11/008)

mHz to kHz gravitational waves with interferometers

Passage of gravitational waves affects the propagation time of laser beam in the arms of an interferometer. Measurement of interference pattern variability allows to detect gravitational waves in the kHz range with km-scale interferometers and down to mHz with 10^9 cm long arms.

$$P = \sqrt{\frac{2\pi R^3}{G_N M}} \simeq 5 \left[\frac{M}{10^1 M_\odot}\right]^{-\frac{1}{2}} \left[\frac{R}{10^7 \text{ cm}}\right]^{\frac{3}{2}} \text{ ms}; \quad \nu = P^{-1}$$

The same Keplerian period formula suggests that mergers of supermassive black holes produce mHz gravitational waves detectable with LISA space-based interferometer while mergers of stellar mass black holes produce kHz gravitational waves detectable with LIGO/VIRGO/KAGRA interferometers.

A sample of $\sim 10^2$ compact object merger events has been detected in three runs (O1, O2, O3) of LIGO-VIRGO. Most are binary black hole mergers, two are binary neutron stars, there is also a black hole – neutron star merger event.

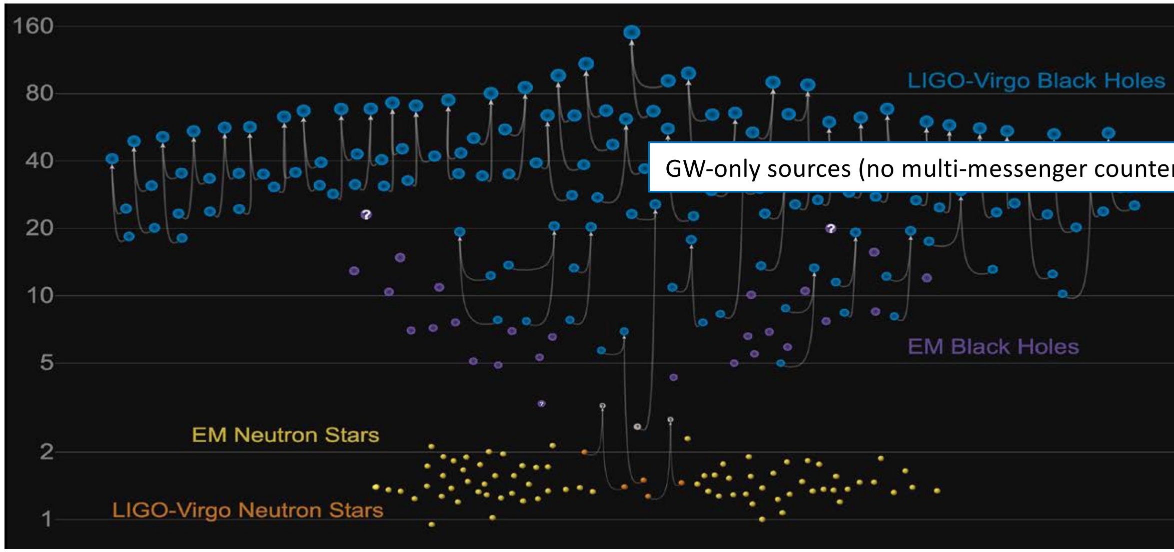

GW150914: LIGO, 2017, PRL, 116, 061102
GW170717: LIGO-VIRGO, 2017, PRL, 119, 161101;

Gravitational waves from neutron star mergers

BH-NS mergers: GW200105 GW200115. No electromagnetic counterpart, but as expected: the NS is not supposed to be tidally disrupted before it plunges under black hole horizon:

$$\frac{\Delta U}{U} \sim \frac{G M_{BH} R_{NS}}{R_{BH}^2} \frac{R_{NS}}{G M_{NS}} \simeq 0.2 \left[\frac{M_{BH}}{5 M_{NS}}\right] \left[\frac{R_{NS}}{R_{BH}}\right]^2$$

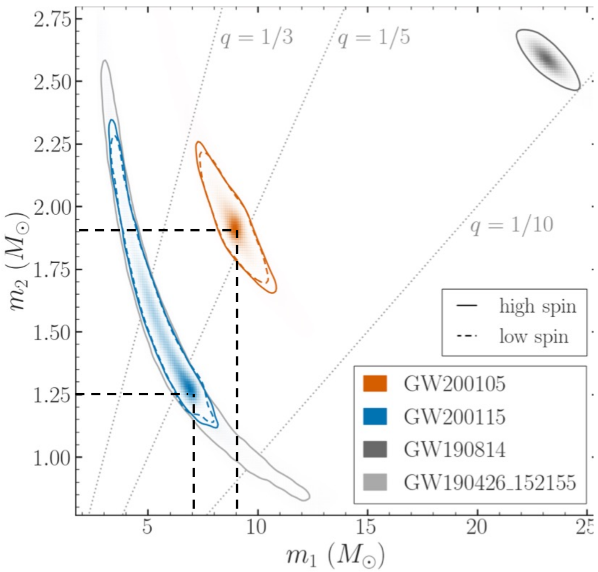

LIGO-VIRGO-KAGRA: 2106.15163

NS-NS mergers: GW170817 GW190425. GW190425 has no detectable electromagnetic counterpart, as expected (distance 160 Mpc,4 times further than GW170817).

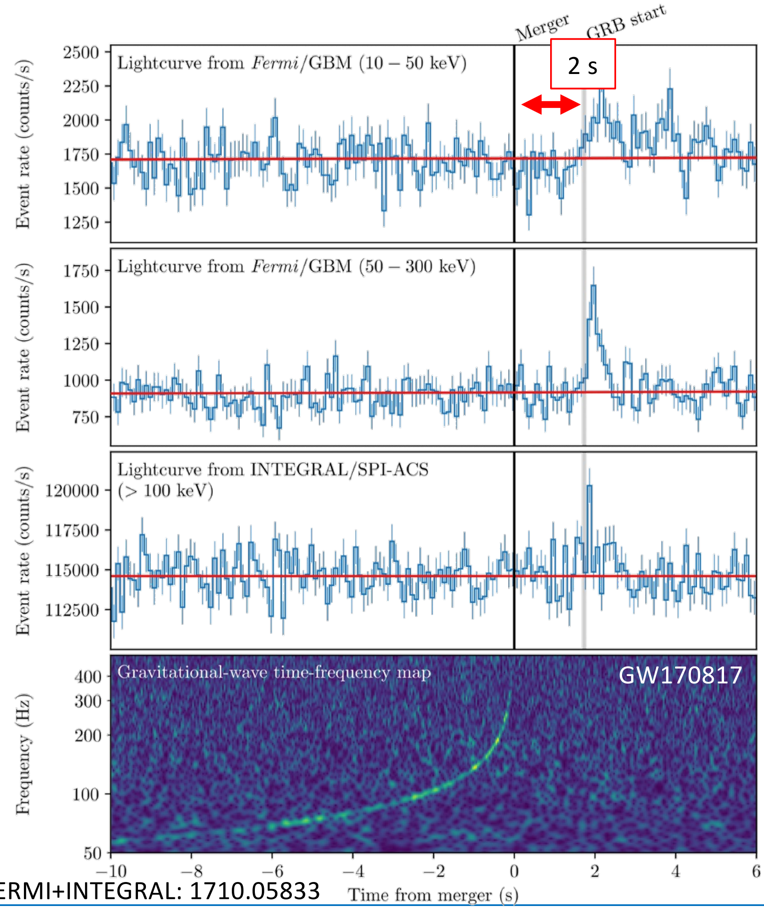

LIGO-VIRGO+FERMI+INTEGRAL: 1710.05833

GW events implications for fundamental physics

Straightforward test of "speed of light vs. speed of gravity": $\Delta v/c \leq 10^{-15}$

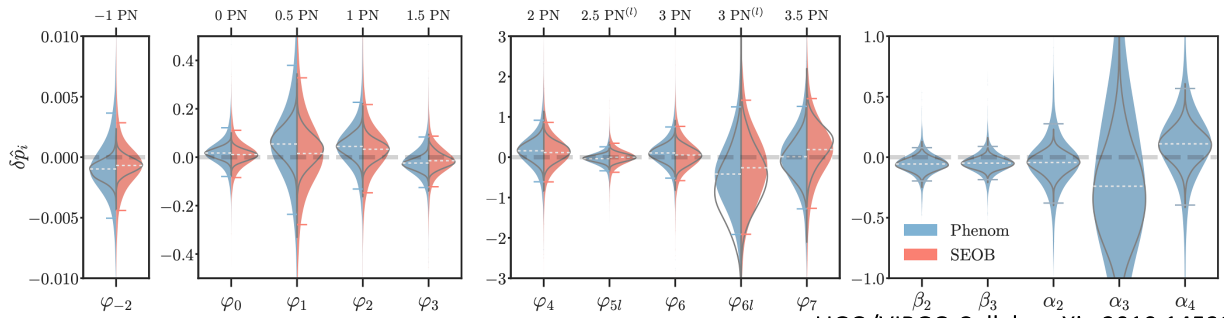

LIGO/VIRGO Collab. arXiv:2010.14529

Constraints on post-Newtonian parameters from O2 run

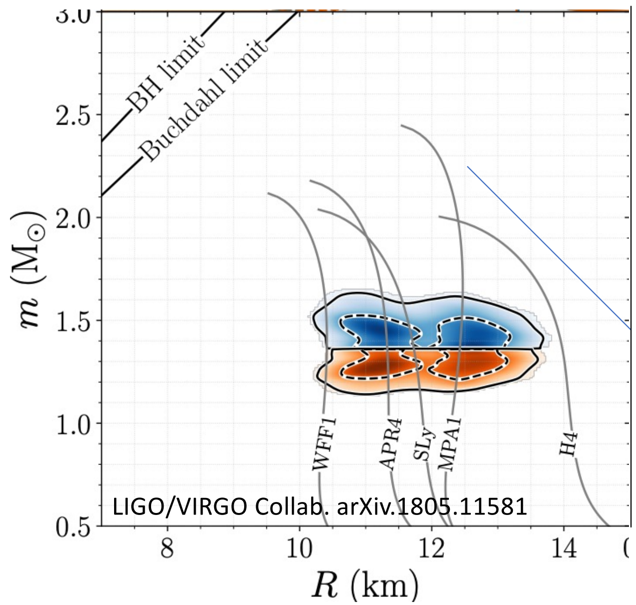

LIGO/VIRGO Collab. arXiv.1805.11581

Tidal deformation of the two inspiraling neutral stars influences the shape of the GW signal. This can be used to constrain the equation of state of nuclear matter inside the neutron stars.

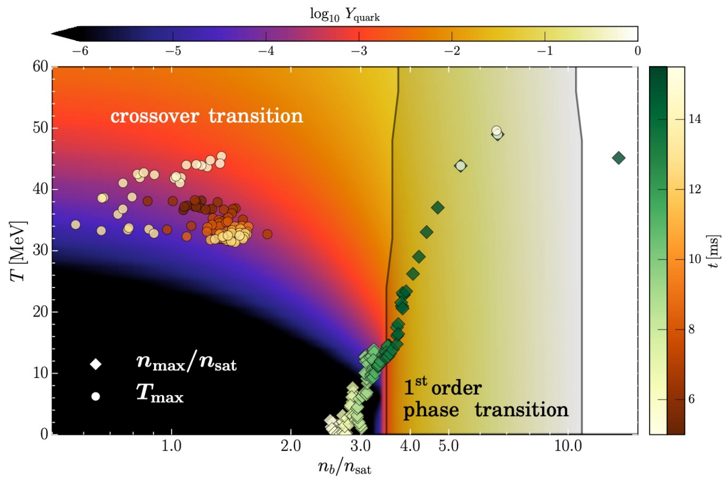

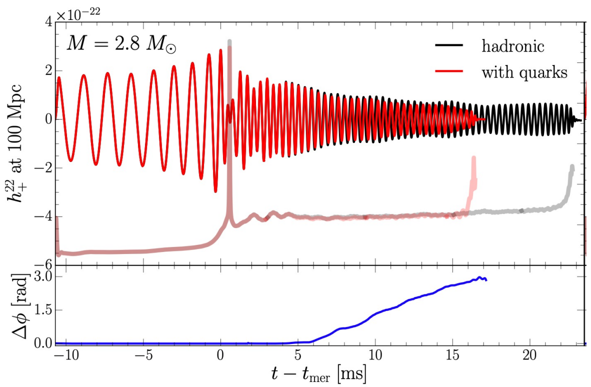

Most et al. arXiv:1807.03684

Post-merger "ring-down" phase waveform is sensitive to possible QCD phase transition that may occur in the collapsing merger object.

Multi-messenger astronomy and the extreme Universe

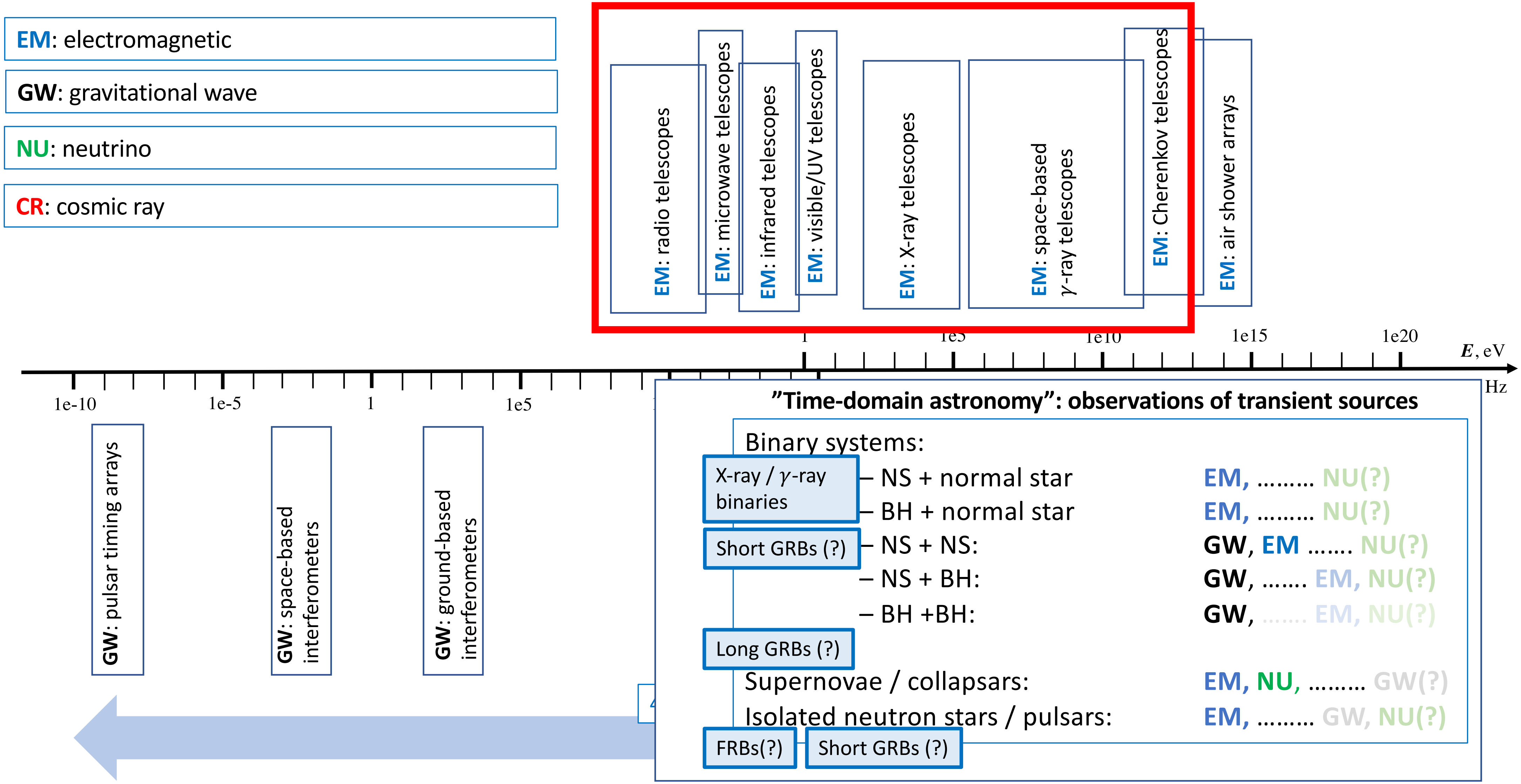

Short gamma-ray bursts (GRB), Fast Radio Bursts (FRB), magnetars

Binary neutron star mergers is one of several possible mechanisms of short GRBs (<2 s spikes of gamma-ray flux). Such mergers produce multi-wavelength “afterglow” emission in radio-visible-X-ray bands due formation of a “kilonova”.

Another type of short GRBs is produced by soft gamma repeaters (magnetars, neutron stars with extremely strong magnetic field, $10^{14} - 10^{15}$G) are known to produce short GRB like giant flares. Flares of magnetars in other galaxies may account of a significant fraction of short GRBs.

Hurley et al. astro-ph/0502329

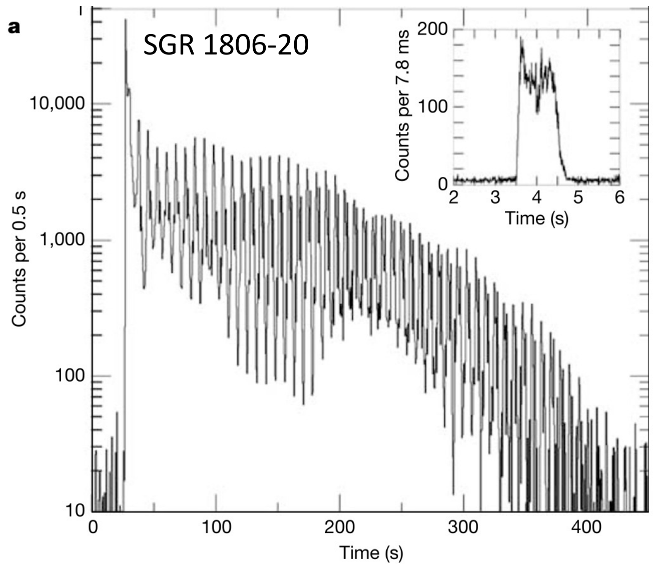

Soft gamma repeater SGR 1935+2154 flare has recently been associated also to another phenomenon: Fast Radio Burst (FRB), $\mu s - \mathrm{ms}$ long spikes of radio flux.

- Before this event only extragalactic FRBs have been detected, no evident counterparts, sometimes repeatedly from the same sky direction.
- Before this event, no magnetar bursts have been associated to radio counterparts…..

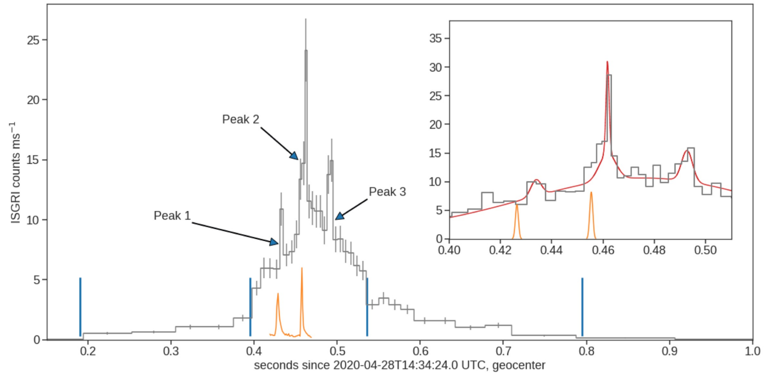

Mereghetti et al., 2005.06335

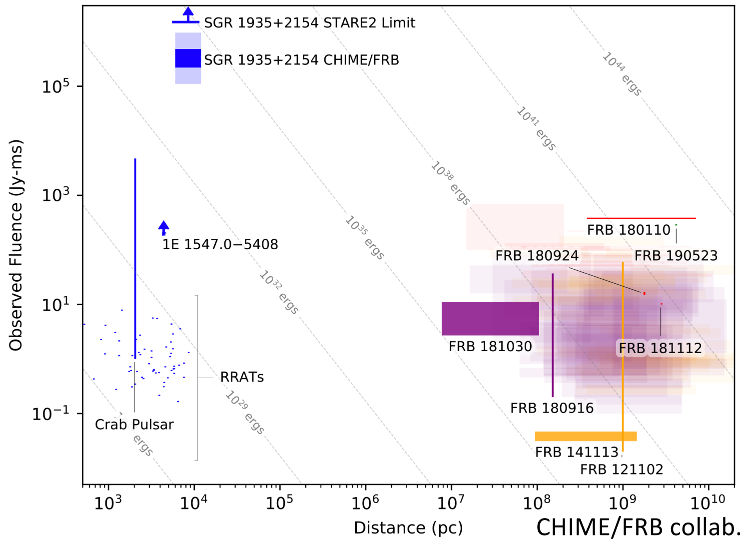

CHIME/FRB collab., 2005.10324.

Core collapse of massive stars, supernovae, long GRBs

Starting from SN 1998bw, Type Ibc supernovae (with progenitor stars stripped of their hydrogen and possibly helium envelope) are associated with long GRBs.

However, recently a long GRB211211A has been associated with a “kilonova”, i.e. the phenomenon produced by neutron star mergers (linke GW170817). This is puzzling, because long/short GRB division was thought to be due to difference in physical mechanisms.

Long GRB afterglow emission is now detected at very-high energies, up to TeV. The emission properties are puzzling: hard spectrum up to several TeV energy, with no signature of cut-off and hard slope of the intrinsic spectra ($\frac{dN_\gamma}{dE} \propto E^{-2}$).

Synchrotron mechanism, possibly responsible for the GeV afterglows observed by Fermi/LAT can hardly explain TeV emission, because energies of electrons accelerated in-situ are limited by the synchrotron loss, limiting the energy of synchrotron photons to be

$$E_{synch} \leq 10^{2.5}\Gamma \text{ MeV}$$

(Γ is the bulk Lorentz factor of the GRB jet during the afterglow).

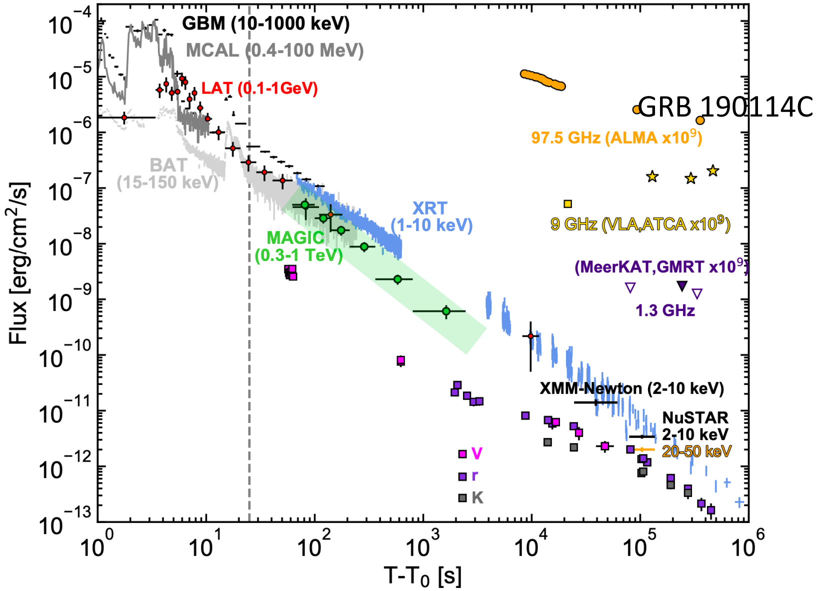

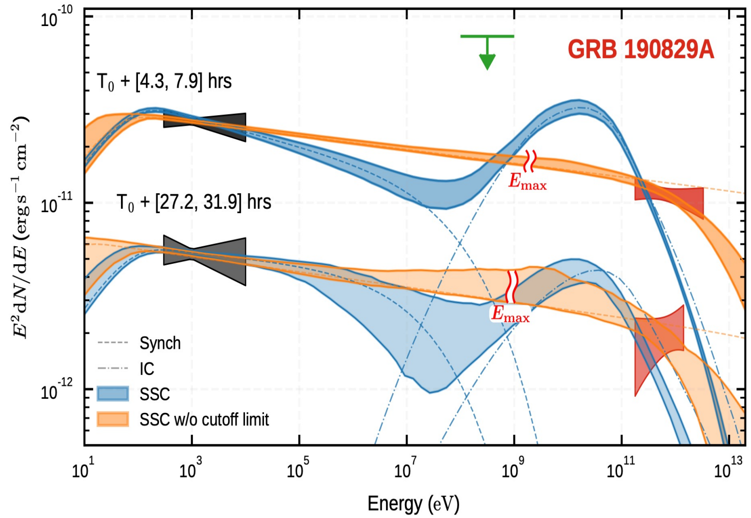

Multi-messenger astronomy and the extreme Universe

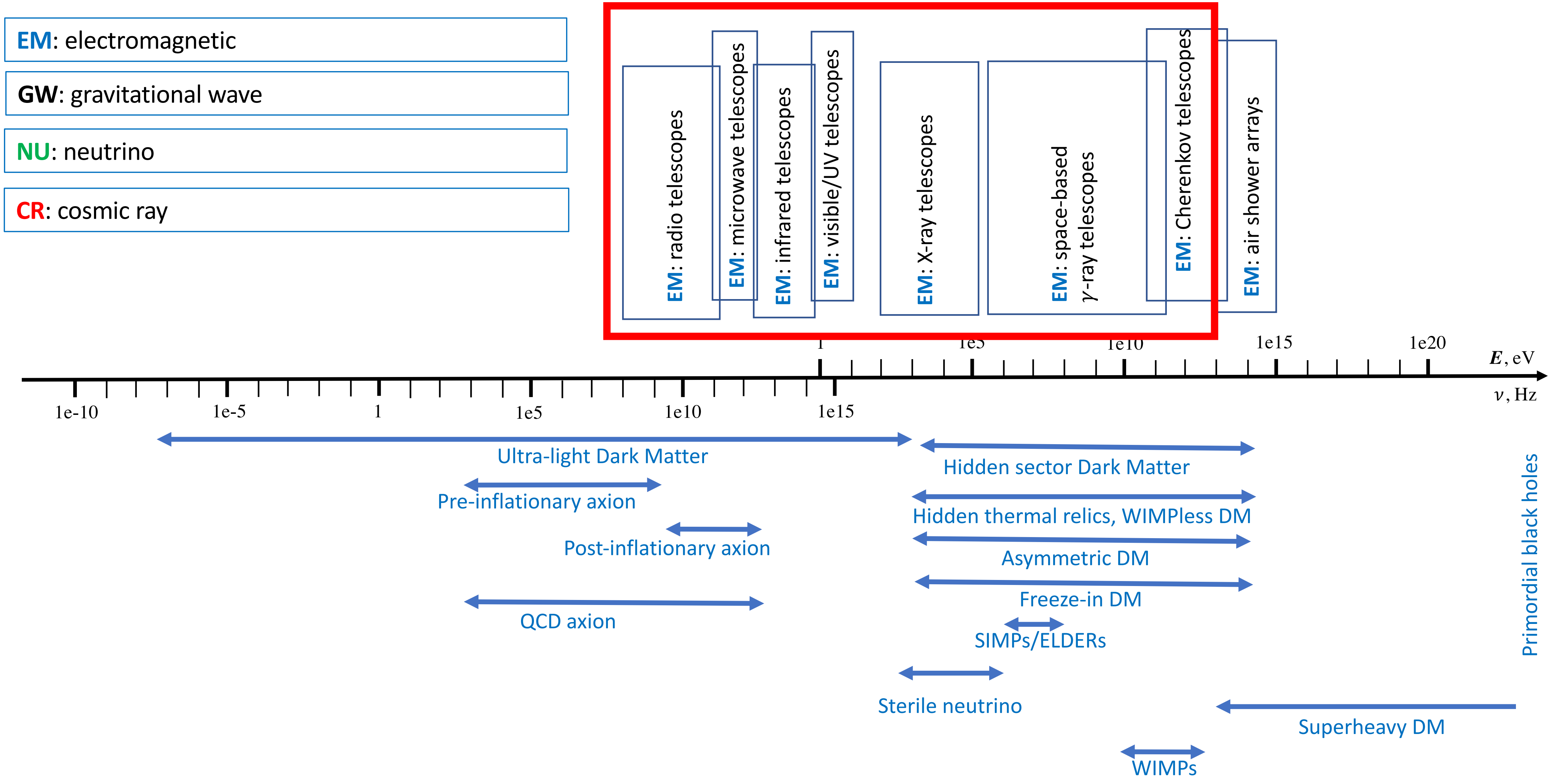

Multi-wavelength probes of fundamental physics (examples)

An excess of extended/diffuse gamma-ray flux (compared to reference diffuse flux model) is observed in Fermi/LAT. It can be interpreted as due to annihilation of WIMPs with thermal relic cross-section.

arXiv:2203.06859

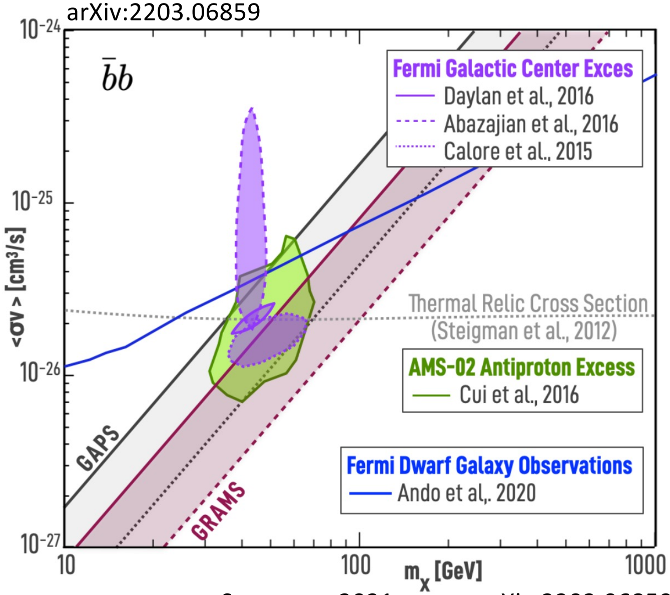

Snowmass2021 paper: arXiv:2203.06859

An excess of visible / infrared Extragalactic Background Light (EBL) is seen by direct measurement experiments and is consistent with constraints from gamma-ray attenuation. It can be interpreted as due to decays of axion-like particles with masses in eV range

Korochkin, AN, Semikoz, 1911.13291

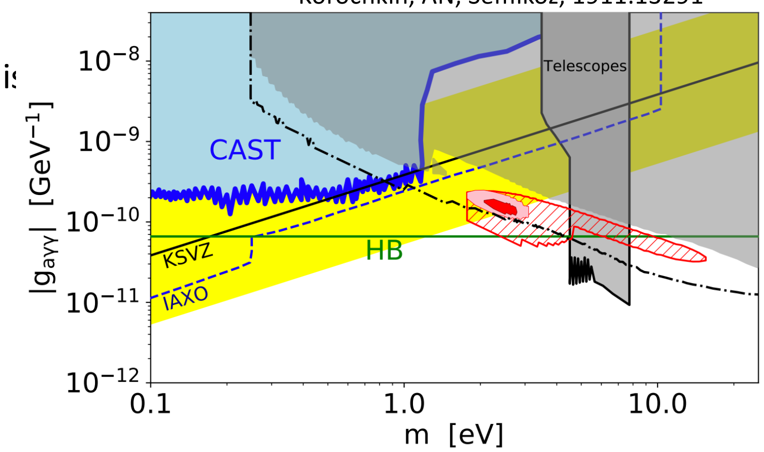

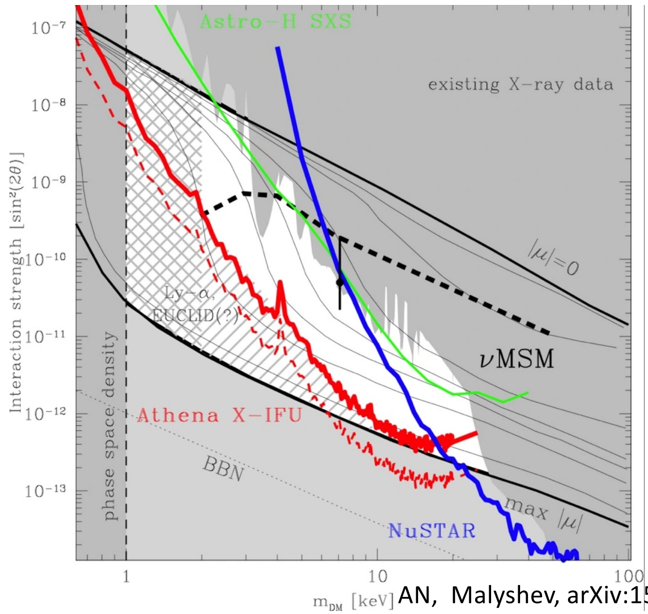

AN, Malyshev, arXiv:1509.02758

“Unidentified” X-ray emission lines in the spectra of galaxies and galaxy clusters (including of diffuse X-ray emission from the Milky Way) can be due to the decaying sterile neutrino dark matter. An evidence for such a line at 3.5 keV is debated.

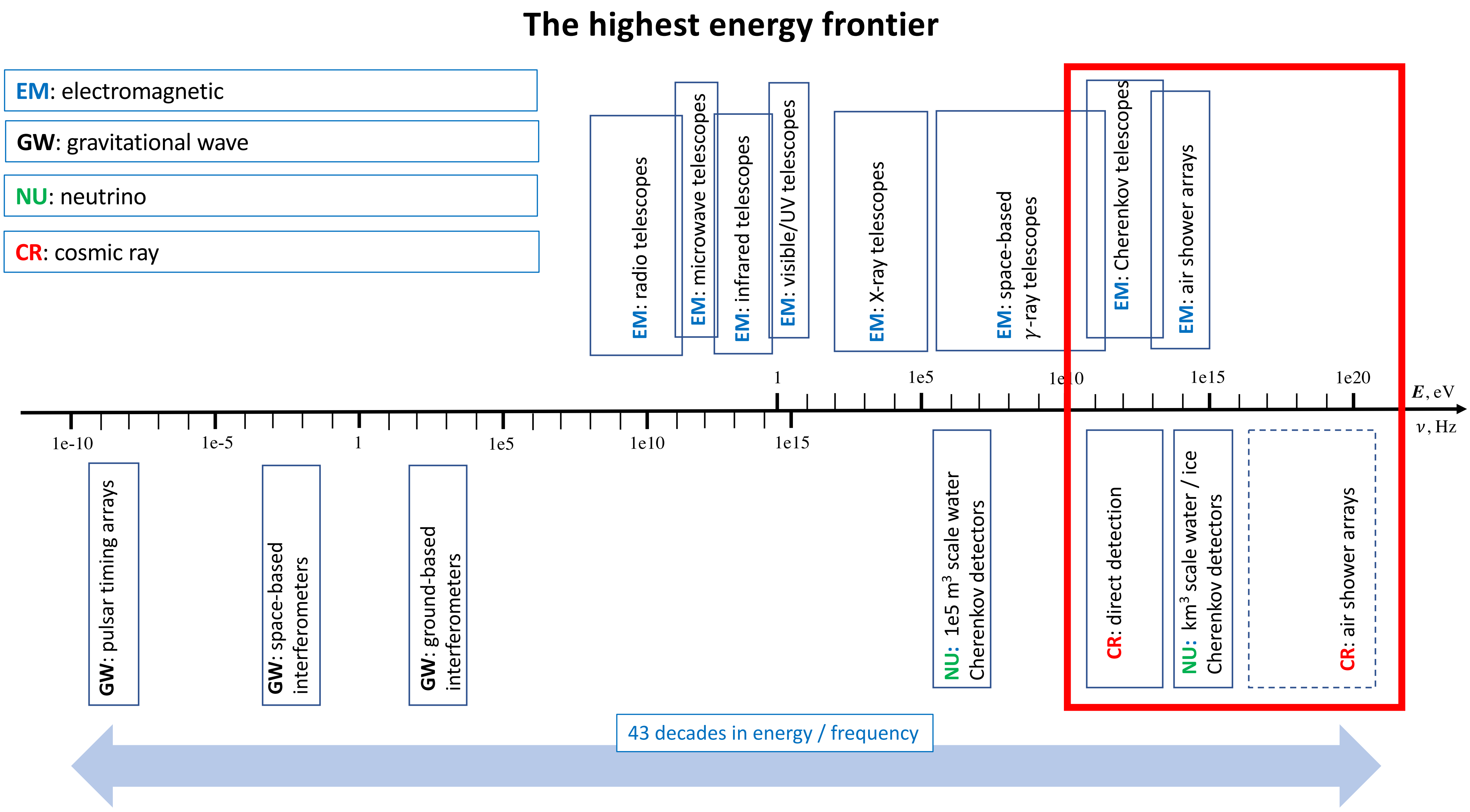
The highest energy frontier
EM: electromagnetic
GW: gravitational wave
NU: neutrino
CR: cosmic ray
EM: radio telescopes
EM: microwave telescopes
EM: infrared telescopes
EM: visible/UV telescopes
EM: X-ray telescopes
EM: space-based γ-ray telescopes
EM: Cherenkov telescopes
EM: air shower arrays
1
1e5
1e10
1e15
1e20
E, eV
ν, Hz
1e-10
1e-5
1
1e5
1e10
1e15
GW: pulsar timing arrays
GW: space-based interferometers
GW: ground-based interferometers
NU: 1e5 m3 scale water Cherenkov detectors
CR: direct detection
NU: km3 scale water / ice Cherenkov detectors
CR: air shower arrays
43 decades in energy / frequency

Astrophysical neutrinos in 10 TeV - 10 PeV range

Large volumes of ice or water are used as Cherenkov detectors to detect tracks of charged particles produced in interactions of high-energy neutrinos.

Baikal GVD and KM3NET (water) are joining IceCube (ice) as km^3 scale detectors. They have comparable performance to IceCube for neutrino detection in muon channel, but better angular resolution in cascade channel.

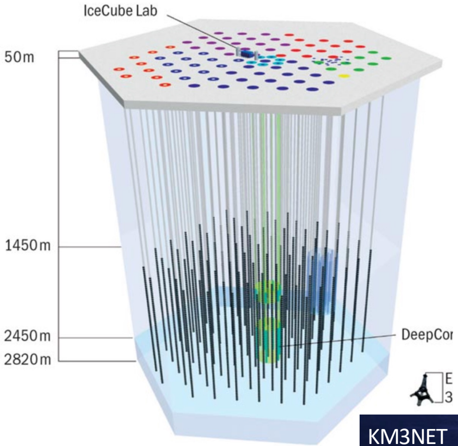

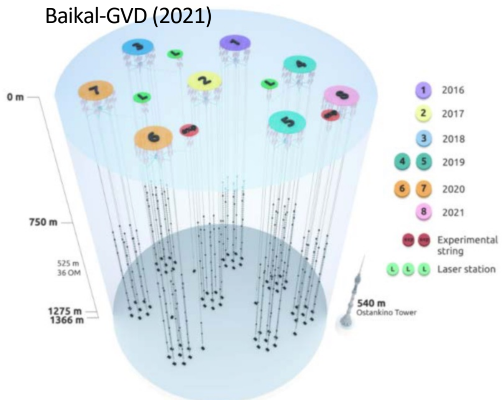

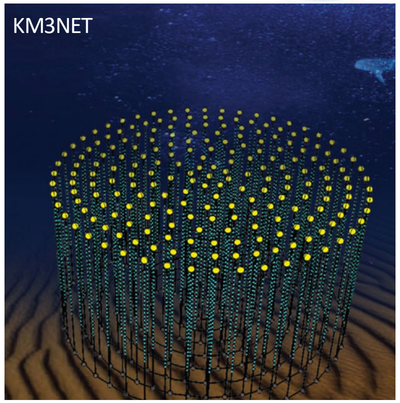

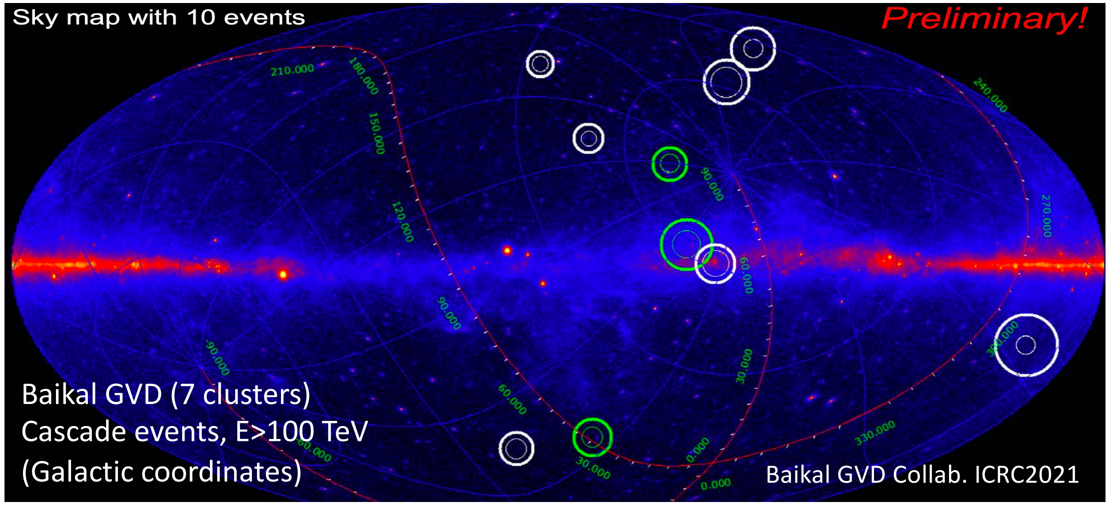

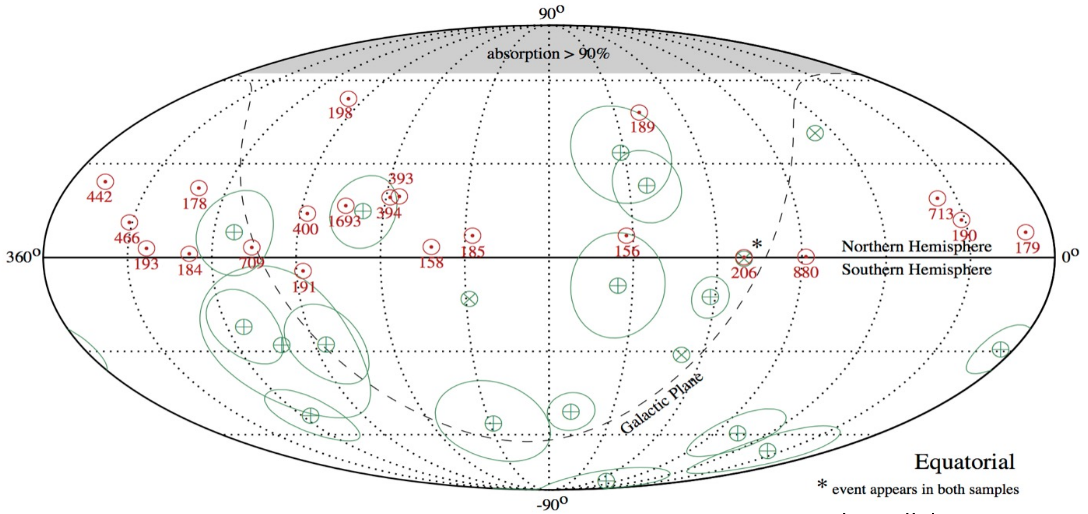

IceCube HESE (cascades and tracks)E>30 TeV
(Equatorial coordinates)

IceCube Collab. 1507.04005

Astrophysical neutrinos in 10 TeV - 10 PeV range

Astrophysical neutrino spectrum measurements in different channels event types and sampled from different parts of the sky reveal powerlaw spectrum $\frac{dN_\nu}{dE} \propto E^{-\Gamma}$ with slope(s) $\Gamma = 2.2\,..\,2.5$. The signal is consistent with being isotropic (considered as an evidence for extragalactic origin of the signal).

An immediate problem for a soft spectrum neutrino signal of extragalactic origin is the absence of the counterpart γ-ray signal at lower energy. Instead, low-energy extrapolation of the neutrino flux is consistent with Galactic diffuse emission γ-ray signal.

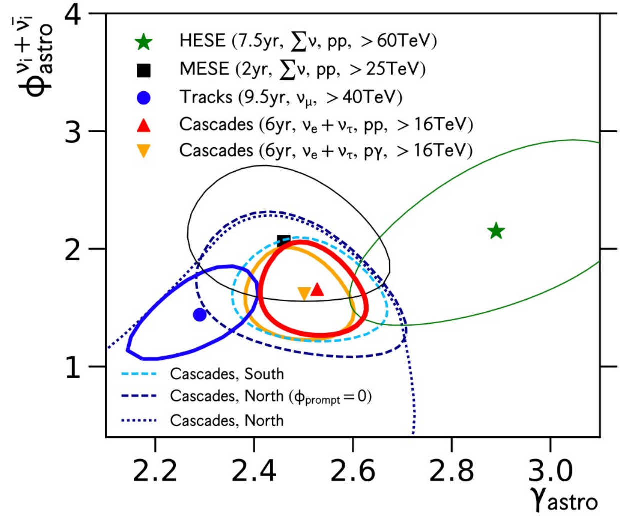

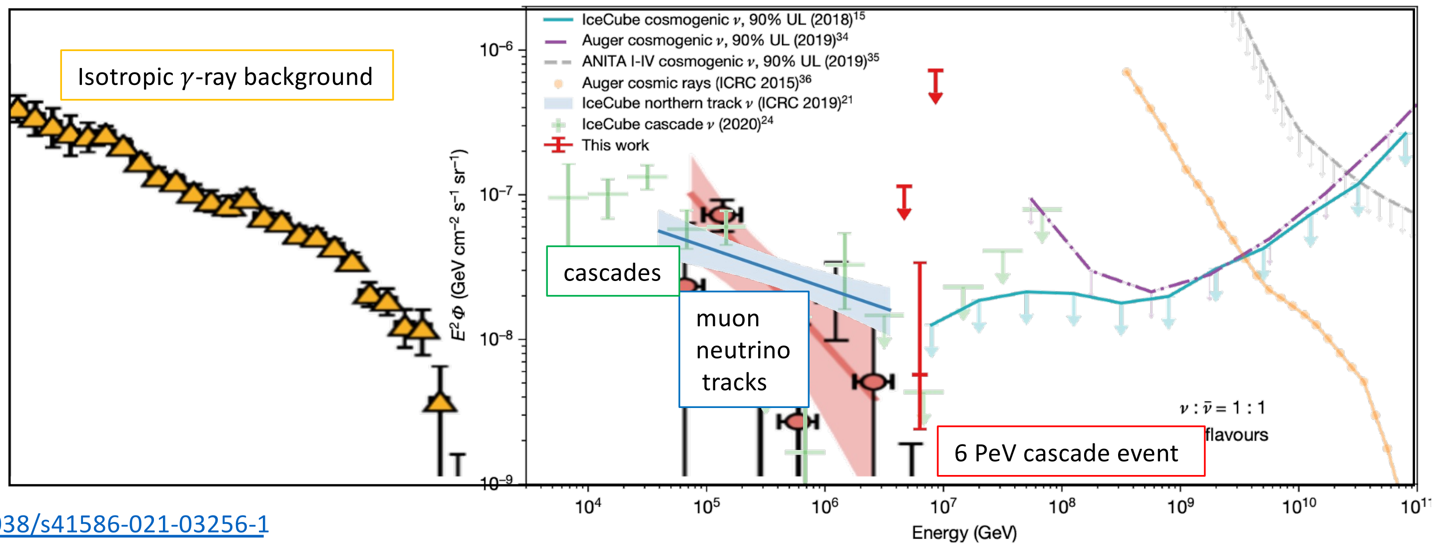

IceCube Collab. 1908.09551, 2001.09520, https://doi.org/10.1038/s41586-021-03256-1

Astrophysical neutrinos in 10 TeV - 10 PeV range

Astrophysical neutrino spectrum measurements in different channels event types and sampled from different parts of the sky reveal powerlaw spectrum $\frac{dN_\nu}{dE} \propto E^{-\Gamma}$ with slope(s) $\Gamma = 2.2\,..\,2.5$. The signal is consistent with being isotropic (considered as an evidence for extragalactic origin of the signal).

An immediate problem for a soft spectrum neutrino signal of extragalactic origin is the absence of the counterpart γ-ray signal at lower energy. Instead, low-energy extrapolation of the neutrino flux is consistent with Galactic diffuse emission γ-ray signal.

The neutrino flux level is, however consistent with the γ-ray flux from the Milky Way.

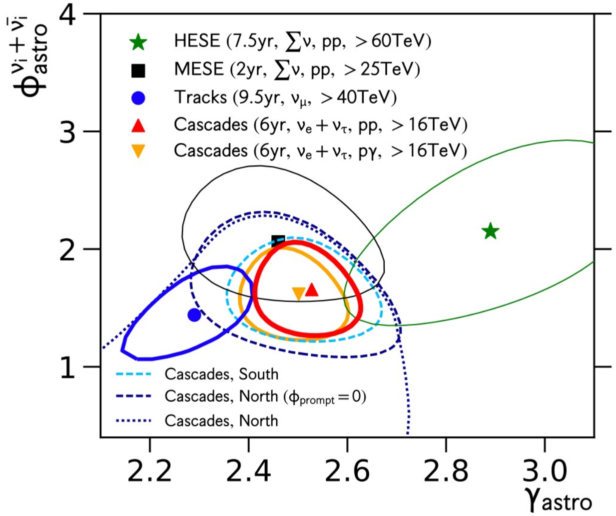

Extension of gamma-ray measurements into the energy range of neutrino signal should help: there is no clear understanding of physics of cosmic ray propagation in the Milky Way and of the origin of the locally observed slope of the cosmic ray spectrum.

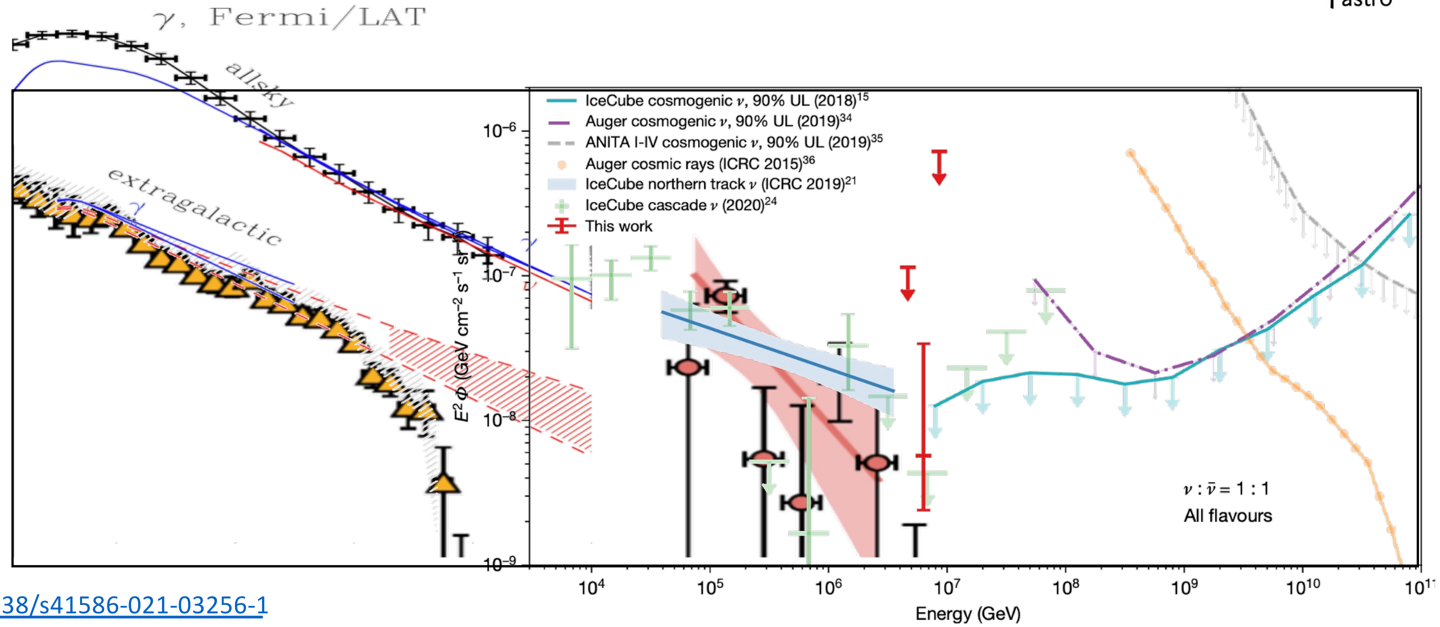

AN, Semikoz 1412.1690, 1907.06061
IceCube Collab. 1908.09551, 2001.09520, https://doi.org/10.1038/s41586-021-03256-1

Gamma-rays with energies up to 1 PeV

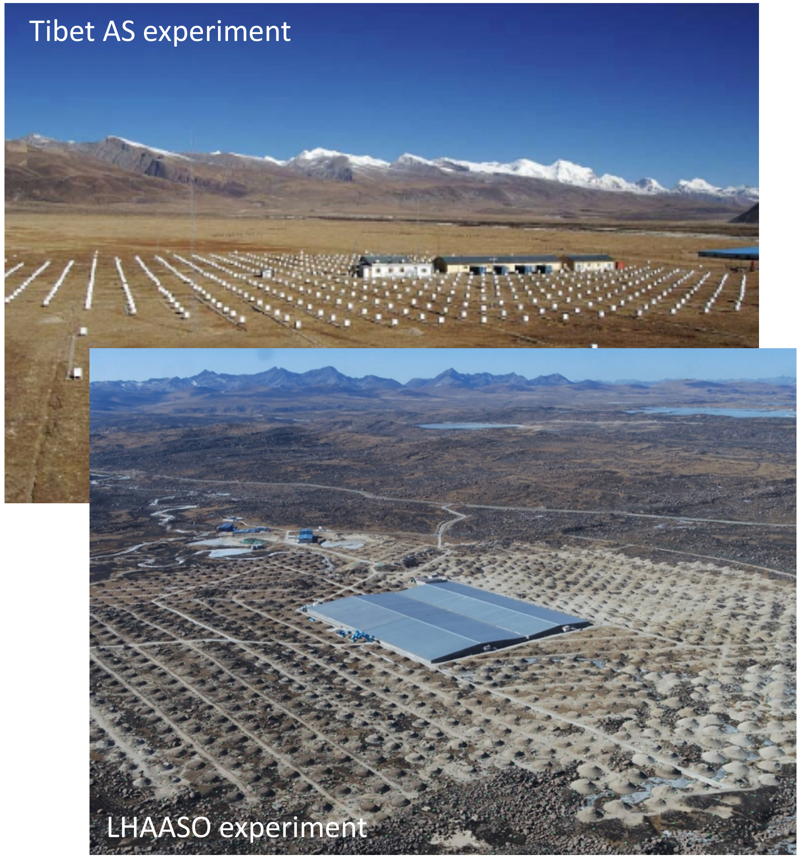

Water Cherenkov detectors, arrays of scintillator counters and muon detectors are used to detect particle air shower induced by γ-rays and distinguish them from background showers produced by proton and nuclei.

Tibet AS γ-ray map E>398 TeV

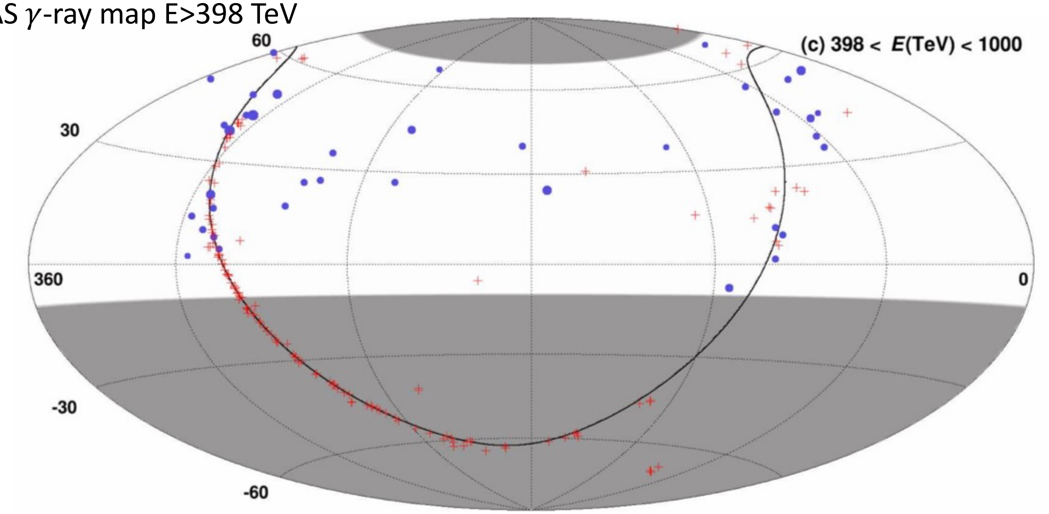

LHAASO sky map E>100 TeV

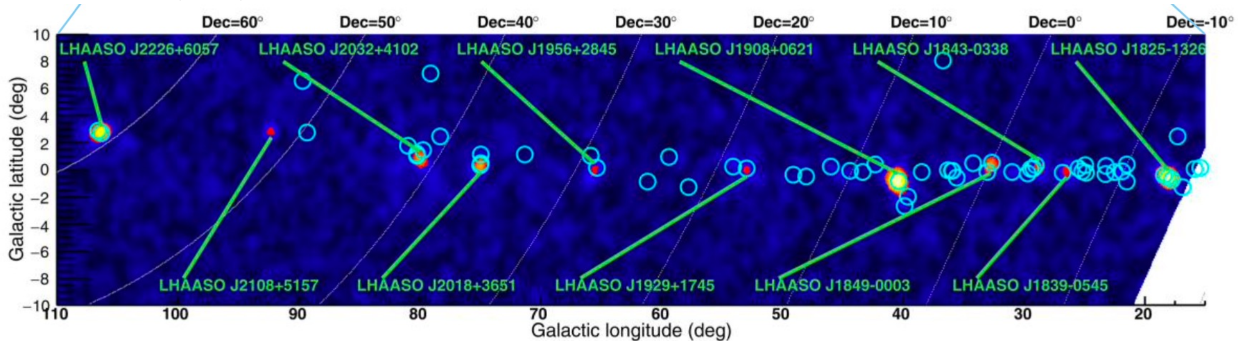

Tibet Collab. 2104.05181

LHAASO Collab. https://doi.org/10.1038/s41586-021-03498-z

Gamma-rays with energies up to 1 PeV

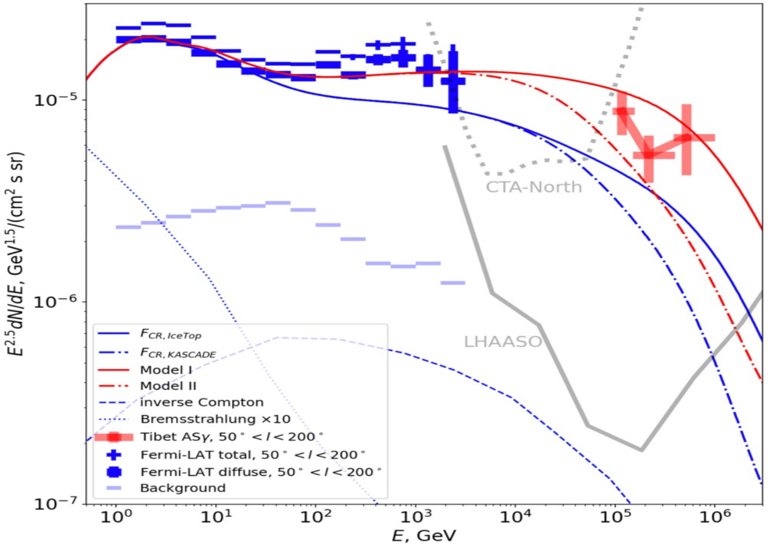

Tibet AS γ-ray map E>398 TeV

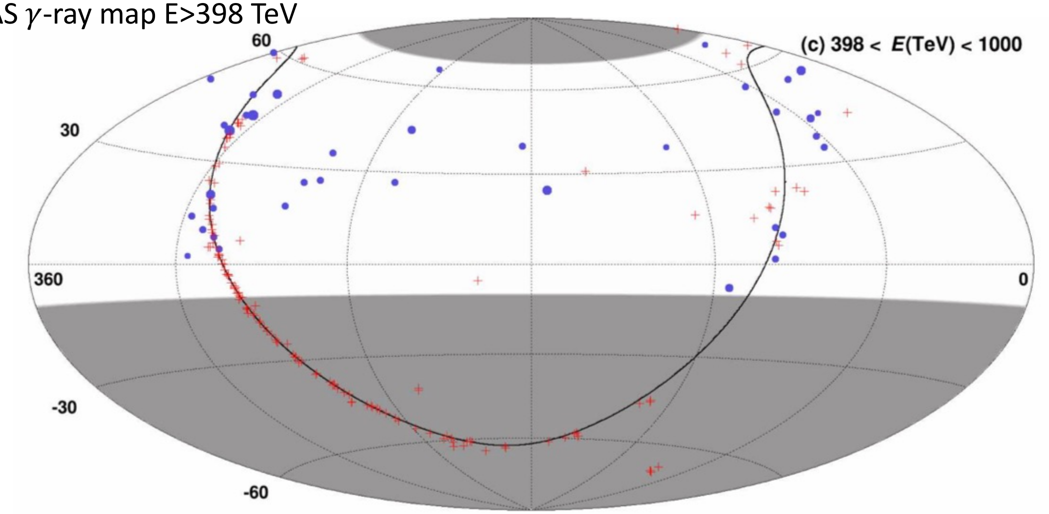

Tibet AS collaboration has reported detection of diffuse emission in the energy range up to 1 PeV (overlapping with that of IceCube neutrino signal) from parts of the Galactic Plane.

Combination of Tibet AS measurements with those of Fermi/LAT telescope suggests that average cosmic ray spectrum is harder than locally measured and has a knee feature.

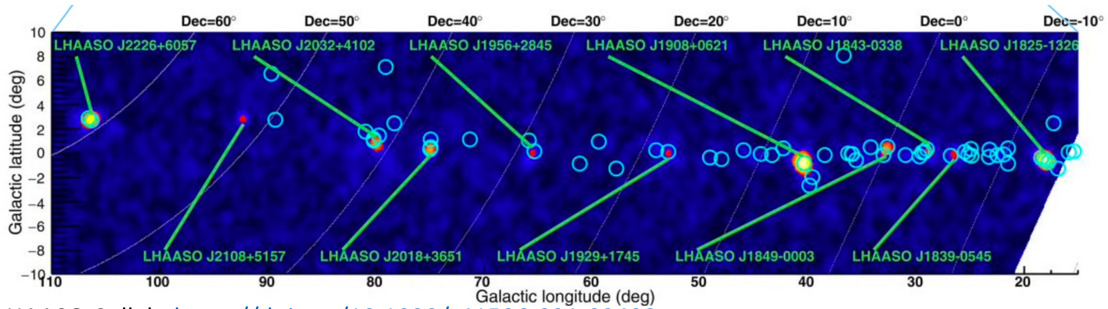

LHAASO Collab. https://doi.org/10.1038/s41586-021-03498-z

LHAASO has reported detection of 12 γ-ray sources in 0.1-1 PeV energy range, with spectra extending into PeV range without cutoffs.

Tibet Collab. 2104.05181
Koldobskiy, AN, Semikoz, 2105.00959,
AN, Semikoz, Vovk, 2107.06541

UHECR astronomical observational window?

Arrays of water Cherenkov detectors and scintillator pads spread over areas up to are used to detect highest energy cosmic rays. Two main experiments: Pierre Auger Observatory (covering 3000 km^2 area) in Southern hemisphere and Telescope Array (upgrading to cover 3000 km^2 area) in Northern hemisphere.

Pierre Auger observatory is currently undergoing an upgrade installing muon detectors and radio antennae network, to improve measurements of identity of primary UHECR particles.

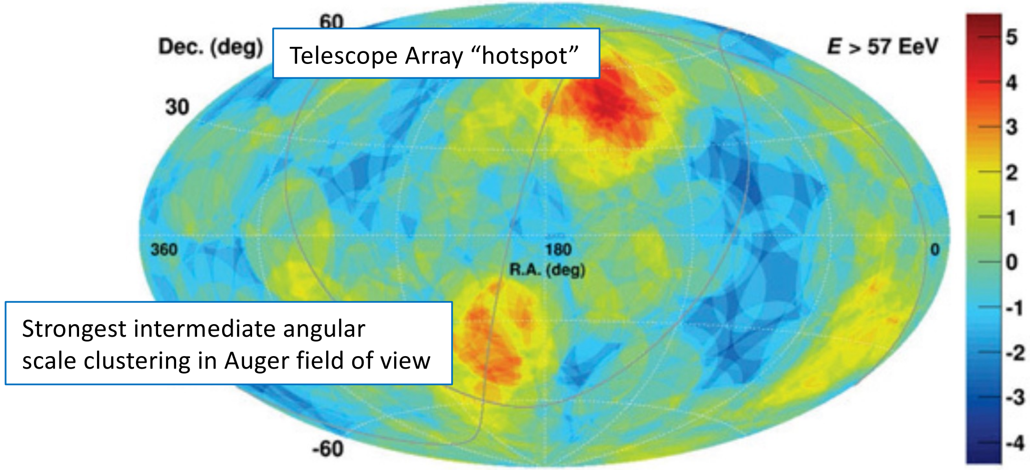

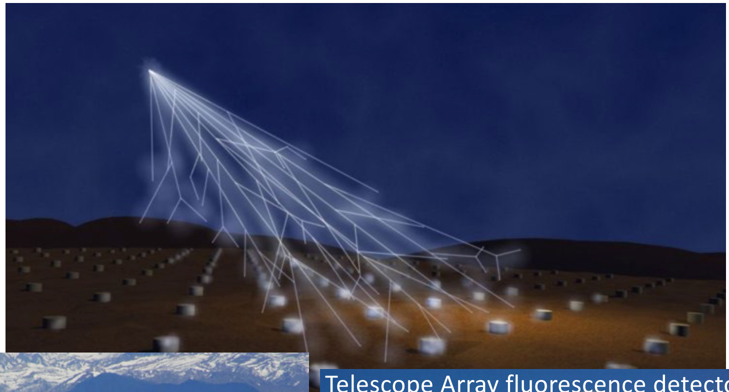


Auger detector unit

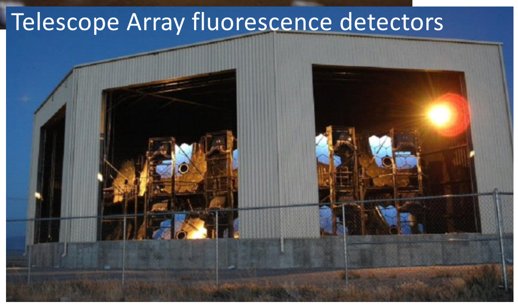
Telescope Array fluorescence detectors

UHECR are charged particles that are only slightly deflected by Galactic magnetic field: $\theta \simeq 1^\circ$ for 10^{20} eV protons. If most of the UHECR are protons, their arrival directions point (almost) to their source location on the sky.

Up to now no isolated sources of UHECR have been detected through analysis of clustering of UHECR arrival directions on the sky.

Large angular scale anisotropy of UHECR arrival directions (dipole) has been detected by Pierre Auger Observatory. Intermediate angular scale anisotropy (20-25 degrees scale) has been reported by both Telescope Array and Pierre Auger Observatory.

Pierre Auger Observatory (public data release): arXiv:2206.13492

UHECR observational window?

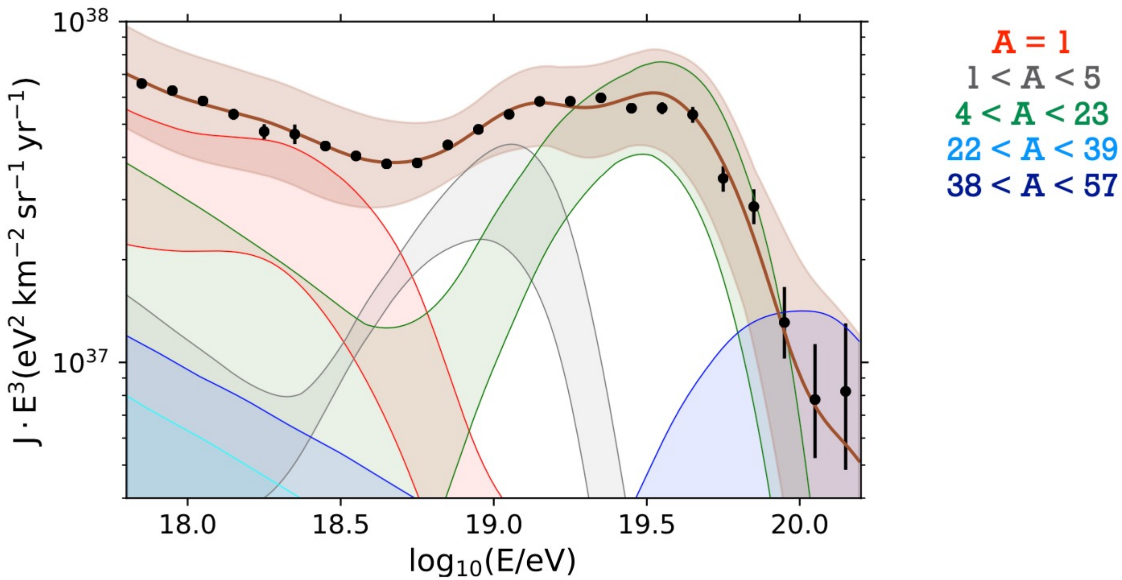

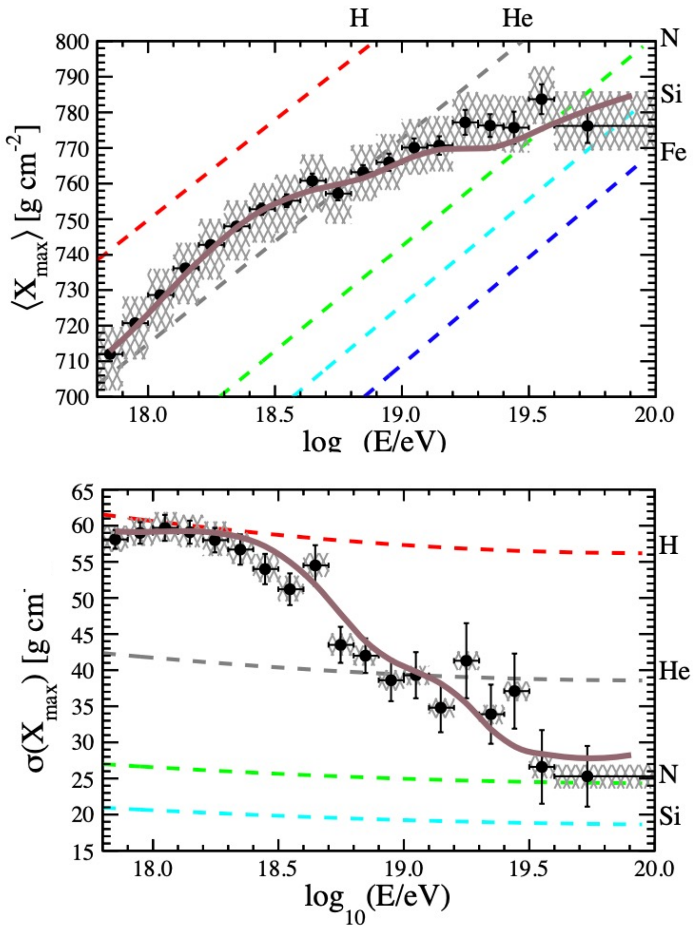

Auger and Telescope array measurements indicate that Northern and Southern sky spectra differ at the highest energy end. The spectra are consistent in the part of the sky visible to both experiments, if cross-calibration is performed (10% level correction of energy scale).

Analysis of composition of UHECR flux by Auger indicates that the highest energy flux is dominated by heavy nuclei. This is not confirmed (yet?) by Telescope Array.

Heavy nuclei composition of UHECR flux complicates clustering analysis aimed at the search of UHECR sources via backtracing of their UHECR arrival directions. Uncertainties of knowledge of Galactic magnetic field strongly affect precision of the analysis.

Pierre Auger Collab. ICRC 2021

Highest energy probes of fundamental physics (examples)

K.Engel et al. (Snowmass2021), arXiv:2203.10074

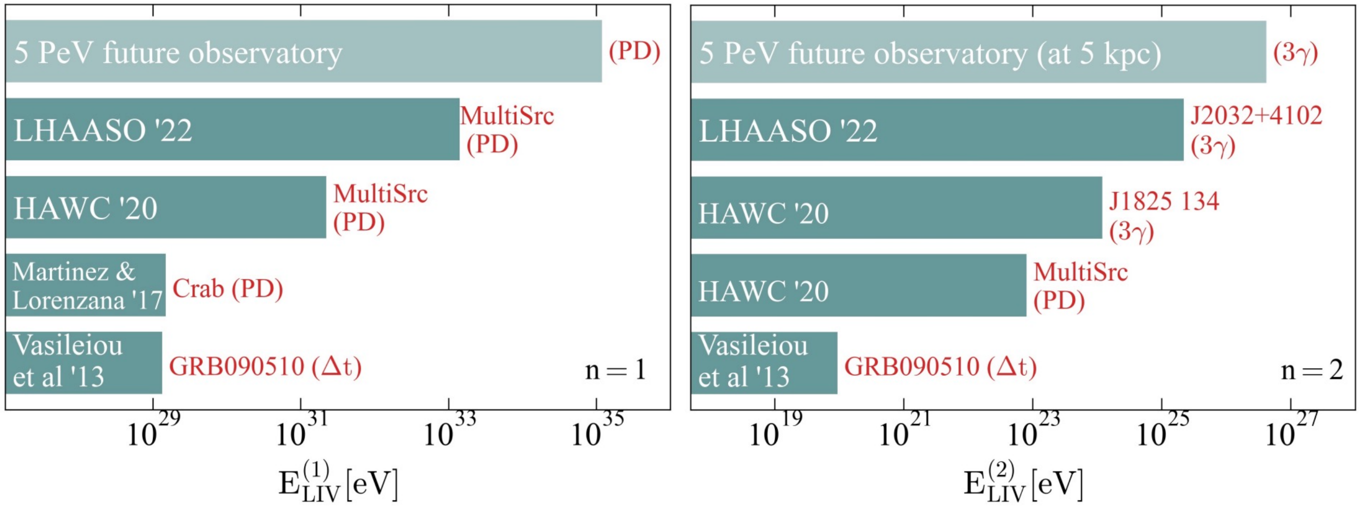

IceCube astrophysical neutrino flux can contain a signal from Dark Matter decays in the Milky Way halo. IceCube limits on anisotropy of neutrino flux and LHAASO mapping of diffuse gamma-ray emission will test this possibility.

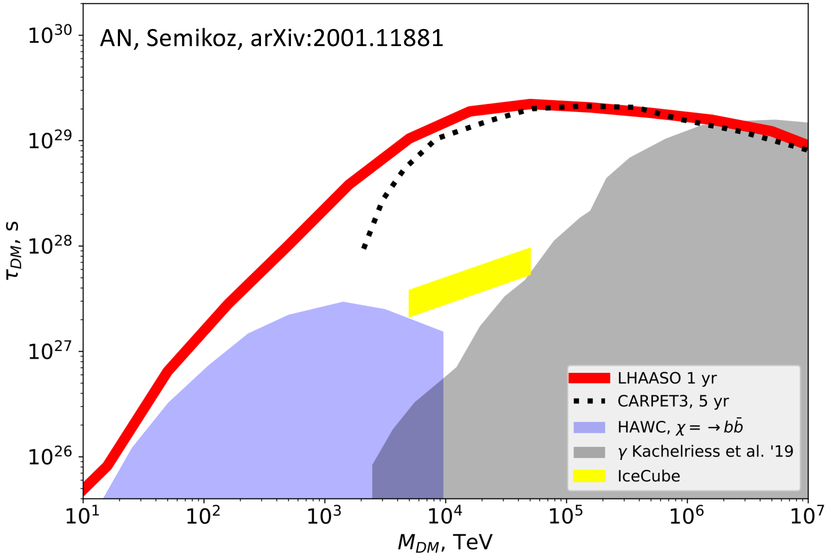

Lorentz invariance violation would manifest itself in the photon dispersion relation $E^2 - p^2 = \pm E^{n+2}/E_{LIV}^{(n)\,n}$ that results in delay / advance of arrival time of higher energy photons. Non-observation of this effect (e.g. in GRB signal) imposes lower bounds on the characteristics energy scales $E_{LIV}^{(n)}$. Modification of the dispersion relation also modifies the thresholds of reactions, specifically of the $\gamma\gamma \to e^+e^-$. Mere observations of the highest energy gamma-rays from astronomical sources imposes lower bounds on $E_{LIV}^{(n)}$.

Summary

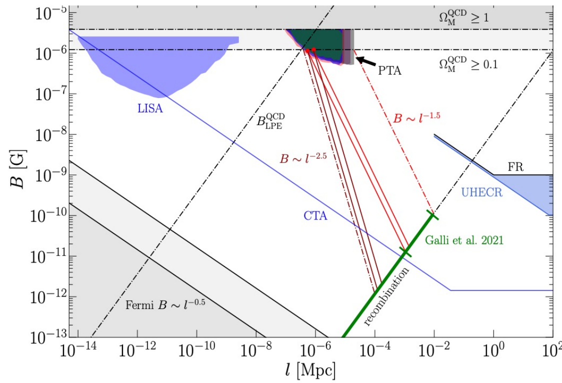
LISA
CTA
UHECR
FR
PTA
Galli et al. 2021
recombination
Fermi $B \sim l^{-0.5}$
$B \sim l^{-2.5}$
$B \sim l^{-1.5}$
$B_{\rm LPE}^{\rm QCD}$
$\Omega_M^{\rm QCD} \geq 1$
$\Omega_M^{\rm QCD} \geq 0.1$
B [G]
l [Mpc]

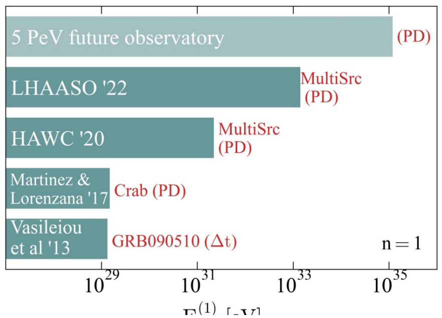
5 PeV future observatory
(PD)
LHAASO '22
MultiSrc (PD)
HAWC '20
MultiSrc (PD)
Martinez & Lorenzana '17
Crab (PD)
Vasileiou et al '13
GRB090510 (Δt)
n = 1

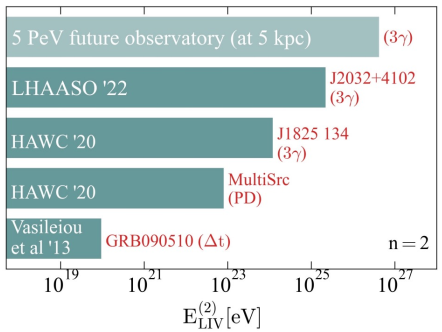
5 PeV future observatory (at 5 kpc)
(3γ)
LHAASO '22
J2032+4102 (3γ)
HAWC '20
J1825 134 (3γ)
HAWC '20
MultiSrc (PD)
Vasileiou et al '13
GRB090510 (Δt)
n = 2
$E_{\rm LIV}^{(2)}$ [eV]

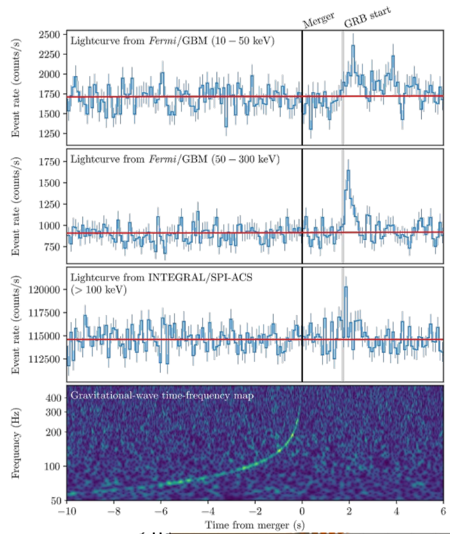
Merger
GRB start
Lightcurve from Fermi/GBM (10 − 50 keV)
Lightcurve from Fermi/GBM (50 − 300 keV)
Lightcurve from INTEGRAL/SPI-ACS (> 100 keV)
Gravitational-wave time-frequency map
Event rate (counts/s)
Frequency (Hz)
Time from merger (s)

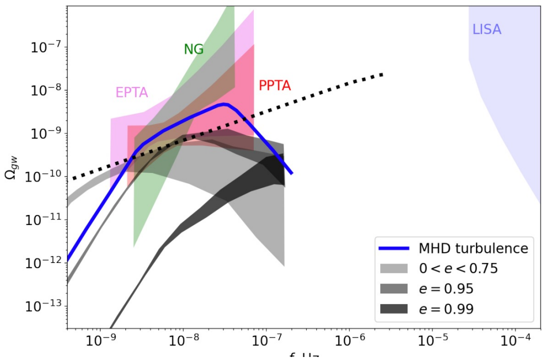
LISA
NG
EPTA
PPTA
Ω_{gw}
MHD turbulence
$0 < e < 0.75$
$e = 0.95$
$e = 0.99$

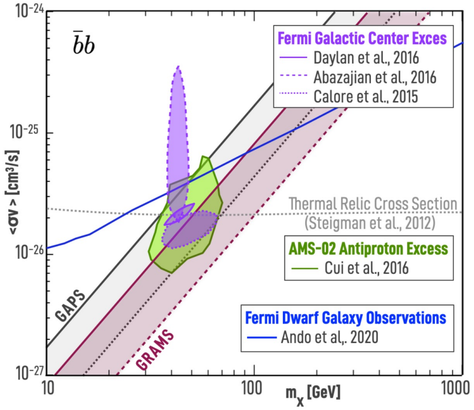
$\bar{b}b$
Fermi Galactic Center Exces
Daylan et al., 2016
Abazajian et al., 2016
Calore et al., 2015
Thermal Relic Cross Section
(Steigman et al., 2012)
AMS-02 Antiproton Excess
Cui et al., 2016
Fermi Dwarf Galaxy Observations
Ando et al., 2020
GAPS
GRAMS
<σv> [cm³/s]
m_χ [GeV]

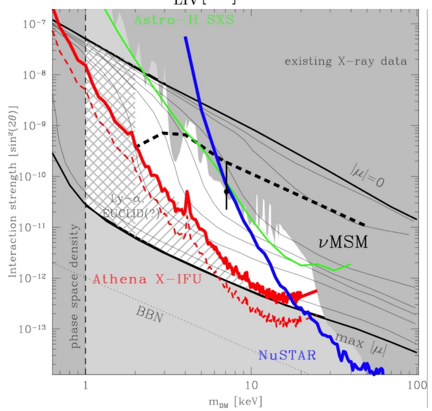
Astro-H SXS
existing X-ray data
νMSM
Athena X-IFU
NuSTAR
BBN
phase space density
interaction strength [sin²(2θ)]
$m_{\rm DM}$ [keV]

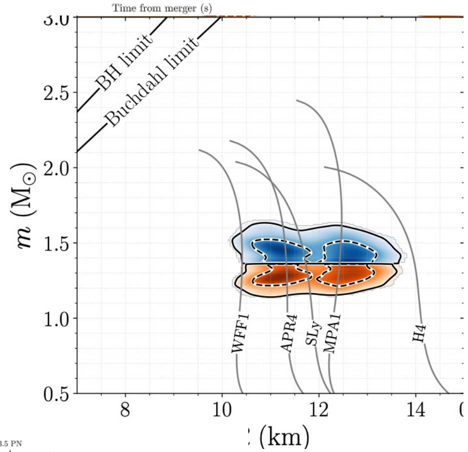
BH limit
Buchdahl limit
WFF1
APR4
SLy
MPA1
H4
m (M⊙)

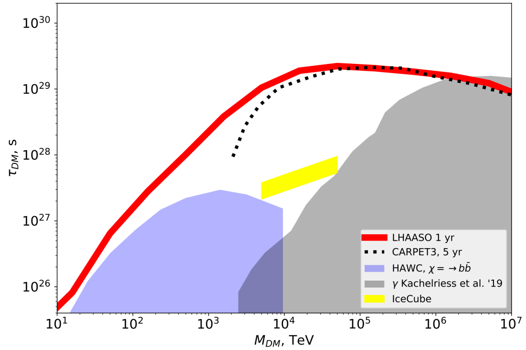
LHAASO 1 yr
CARPET3, 5 yr
HAWC, $\chi \to b\bar{b}$
γ Kachelriess et al. '19
IceCube
τ_{DM}, s
M_{DM}, TeV

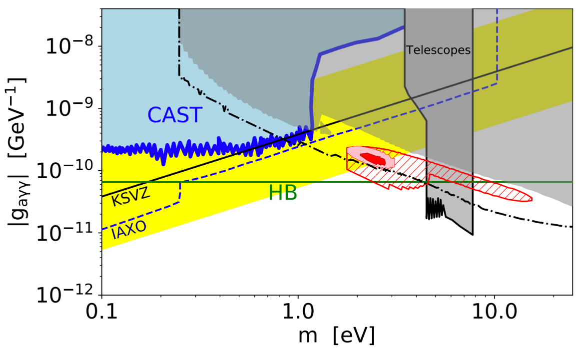
CAST
Telescopes
KSVZ
IAXO
HB
$|g_{a\gamma\gamma}|$ [GeV^{-1}]
m [eV]

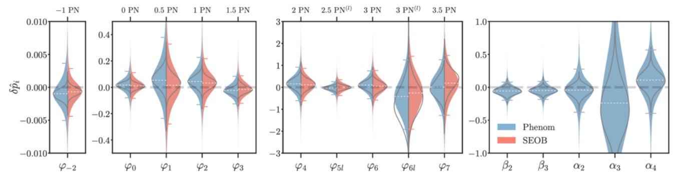
Phenom
SEOB